JOINT EUROPEAN TORUS JET

JET–P(87)08

O.N. Jarvis, G. Gorini, J. Källne, V. Merlo, G. Sadler,
P. van Belle and the JET Team

Determination of the Deuterium Plasma Density Ratio n_d/n_e Through Neutron Measurements

Determination of the Deuterium Plasma Density Ratio n_d/n_e Through Neutron Measurements

O.N. Jarvis, G. Gorini, J. Källne, V. Merlo, G. Sadler,
P. van Belle and the JET Team

JET-EFDA, Culham Science Centre, OX14 3DB, Abingdon, UK

Preprint of Paper to be submitted for publication in
Nuclear Fusion Journal

JET-P(87)08

DETERMINATION OF THE DEUTERIUM PLASMA DENSITY RATIO $\hat{n}_d/\hat{n}_e$ THROUGH NEUTRON MEASUREMENTS

O N Jarvis, G Gorini, J Källne, V Merlo,
G Sadler and P van Belle

JET Joint Undertaking, Abingdon, Oxon OX14 3EA, UK

ABSTRACT

JET has been operating with deuterium plasmas for the past two years, during which time neutron spectrometry has been applied as a diagnostic technique for determining the ion temperature for suitable discharges. Only ohmically heated discharges and those with ICRF additional heating provide the necessary thermal equilibrium in the deuterium ions for a simple interpretation of the neutron energy spectra to be possible. Furthermore, only plasma discharges generating in excess of 10^{12} neutrons per second provide a sufficiently strong signal for the statistical accuracy of the measurement to be useful. Combining the "neutron temperature" with the neutron yield determination made with a fission counter diagnostic permits the central deuteron to electron density ratio $(\hat{n}_d/\hat{n}_e)$ to be determined. It is found that this ratio, for Ohmically heated discharges, appears to fall with ion temperature from about 70% at 2keV to 40% at 3keV. This result can be expressed in a more familiar way by stating that Z_{eff} increases from 2.5 to 4.5 over this temperature range. The addition of ICRF heating does not alter the density ratio. These findings are consistent with the observation that high temperatures achieved with Ohmic heating in Tokamaks are correlated with high impurity levels.

Submitted for Publication to Nuclear Fusion Journal

1. Introduction

Two neutron diagnostic systems are used on the JET tokamak, one for the measurement of the fusion reaction rate and the other of the central ion temperature for deuterium plasma discharges under conditions of Ohmic heating, supplemented (perhaps) with ICRF additional heating with H or ^{3}He minority ions. Under such conditions the deuterium ions are expected to be in thermal equilibrium, an assumption which is necessary for the discussion presented below.

The first of the diagnostic systems involves the measurement of the yield of neutrons from the d + d → n + ^{3}He reaction and, in some form or other, is a standard measurement for all levels of neutron emission on tokamaks world wide. The second diagnostic, involving ion temperature measurements with a neutron spectrometer on a per discharge basis, is unique to JET but nonetheless is restricted to high neutron yield discharges (> 10^{12} neutrons emitted per second).

As is well-known, the total neutron emission rate is given by $Y_n \sim \int n_d^2 \langle\sigma v\rangle \, d^3x$, where the integral is taken over the whole plasma volume. The reactivity, $\langle\sigma v\rangle$, is strongly temperature-dependent, varying as T_i^α where $\alpha \sim 4$ at T_i = 3keV. The neutron diagnostics determine independently both Y_n and T_i. If it can be assumed that the radial dependencies of the deuterium ion density and temperature are the same as those measured for electrons (which, whilst not strictly correct, should be an acceptable approximation) then the remaining unknown quantity, the central deuterium ion density $\hat{n}_d$, can be determined. For convenience, we express this quantity in ratio form as a density ratio $\hat{n}_d/\hat{n}_e$.

2. Fusion Reaction Rate Measurements

The 2.5MeV neutrons emitted in one of the two branches of the d-d fusion reaction are recorded with three pairs of ^{235}U and ^{238}U fission chambers supported from the vertical limbs of the poloidal field magnet yoke at the level of the horizontal midplane. Neutrons emitted

from the plasma discharge are essentially confined by the massive structure surrounding the vacuum vessel and those which escape must do so through one of the several openings, of which the horizontal diagnostic ports are the largest. Some of these escaping neutrons will scatter from the port windows into the direction of the fission chambers.

The ^{235}U fission chambers, employing polyethylene moderator and substantial lead shielding, have been designed to give a fairly flat response with neutron energy [1]. The variation of the fission chamber response with position of the neutron emitting volume element in the plasma varies considerably around the torus. Accordingly, this variation has been measured [2 3] with the aid of ^{252}Cf radioisotope and 14MeV pulsed tube neutron sources placed inside the JET vacuum vessel. It is implicit in the following that the effects of changes in plasma shape and position on the fission chamber response are always taken into account.

The quantitative relationship between the neutron emission from a plasma discharge (for which the relevant plasma parameters are known) and the response of the fission chamber has been determined to a precision of ± 10% at a neutron flux level corresponding to a total source strength of 10^8 neutrons/sec. The fission chambers are operated in both pulse-counting and current sampling modes but for the work reported here the flux level remained within the operational range of the pulse-counting mode so that response linearity need not be questioned.

3. Neutron Spectrometry

The neutron spectrometer used in this work [4] was a commercial ^3He ionization chamber [5] located in the Roof Laboratory at JET so as to view the centre of the plasma at a distance of 20m vertically below. The shielding was excellent but the collimation was necessarily severe so that only the most intense of Ohmically heated discharges provided useful neutron fluences.

The neutron energy spectrum from a plasma in thermal equilibrium is very nearly Gaussian in form, with a width which gives the ion temperature directly, through the relationship [6]) fwhm = 82.5 $\sqrt{T_i}$, with fwhm and T_i in keV. The recorded energy spectrum is representative of a line-integral through the plasma, albeit heavily weighted to the plasma core. The resultant energy spectrum remains Gaussian but is somewhat narrowed. The correction [6]) to be applied to the line-averaged $\bar{T}_i$ to obtain the central value $\hat{T}_i$ is 1.09 ± 0.01 for all realistic radial dependences of T_i and n_d, provided only that T_i is the more strongly peaked.

The experimental pulse-height spectra are, of course, rather broader than the neutron energy spectra because of the finite resolution of the ^{3}He spectrometer itself. The spectrometer response function for monoenergetic neutrons takes the form of a narrow (40keV fwhm) Gaussian full-energy peak with a small amplitude (5%) tail extending to low energies which is attributed to a detector wall effect. The experimental pulse-height spectra have been fitted [7]) using a minimum likelihood method to curves generated from the convolution of the measured response function and a pure Gaussian, with Gaussian fwhm and amplitude as the only significant variables. A correlated error analysis is performed to obtain the uncertainty in the fwhm and, therefore, in $\hat{T}_i$.

The analysed pulse-height distributions have all been fitted successfully with no significant deviations from Poisson statistics being observed. Because [4]) of the low energy tail to the response function, about 700 counts in the full energy peak are required to give a 10% accuracy in $\hat{T}_i$. To obtain this count it was frequently necessary to perform a sum over repeated, 'identical', discharges. Discharges for which the neutron fluence was insufficient to provide better than 25% statistical accuracy (< 100 counts) were not analysed since it is rare that discharges are repeated more than a few times without altering plasma conditions. In addition to the purely statistical uncertainty, there is also a systematic uncertainty related to the particular choice of spectrometer response function. This was assumed to be energy independent in view of the very narrow

neutron energy range explored (2.45 ± .15MeV). The systematic uncertainty in $\hat{T}_i$ is estimated to be ± 5% and is not temperature dependent.

4. Ion Temperature Data

Over the two years during which JET has been operating with deuterium plasmas there have been only about 50 Ohmic and ICRF-heated discharges of sufficient neutron emission intensity and plasma current flat-top duration to warrant analysis of the neutron spectrometer pulse height data. As shown in Table 1, most of these discharges provided statistical uncertainties in $\hat{T}_i$ which are in excess of 15% but, because several similar discharges were run consecutively, it was possible to improve the accuracy by aggregating the data. In some instances the plasma discharges were intentionally not quite identical so that wherever feasible the data were analysed on a single discharge basis and derived quantities such as $\hat{n}_d/\hat{n}_e$ were averaged afterwards. Of course, the averaged $\hat{T}_i$ for a group of discharges was always independent of whether individual results were averaged or all the spectra were summed and a single averaged temperature derived. The averaged plasma parameters for each group of discharges are presented in Table 1. Mostly, the Table includes only discharges of duration sufficient to ensure steady-state equilibrium between electron and ion temperatures, although Group 6 is a notable exception.

Since neutron spectrometry cannot yet be regarded as an established method of measuring ion temperatures, it is necessary to inspect the data carefully for consistency with other measurements. A comparison of ion temperature measurements is provided in a separate paper [8]) where it is shown that the agreement with results from the Neutral Particle Analysis technique [9]) and from the X-ray crystal spectrometer [10]) is very good over the temperature range from 2 to 5keV, this latter value being achieved using hydrogen neutral beam heating. To be useful in establishing a density ratio temperature dependence, the ion temperatures should be accurate to about 5% - a challenging requirement. Notwithstanding the relative precision of the different diagnostic methods, the neutron spectrometer temperature is strongly preferred for density ratio determinations because it is mostly sensitive to the high-energy tail of the deuteron ion-energy

distribution which, after weighting by the d-d fusion reaction cross-section, is also responsible for the major part of the neutron emission strength. In this specific context all other techniques for measuring ion temperatures are less appropriate and may be subject to problems of interpretation. However, the fact that the three measurement techniques provide similar values of T_i can be taken as good evidence that the energy distribution of the bulk plasma deuterium ions is essentially Maxwellian.

A comparison of the neutron ion temperature $\hat{T}_i$, with the central electron temperature, $\hat{T}_e$, is shown in Fig 1. The essential observation is that $\hat{T}_i$ increases with $\hat{T}_e$, lagging by about 0.6keV for Ohmically heated plasmas. However, remembering the ± 10% normalization uncertainty associated with the electron temperature data and the ± 5% uncertainty for the ion temperature data, it is clearly impossible to draw firm conclusions regarding the temperature differences.

5. The Dilution Factors

Given reliable $\hat{T}_i$ data, the neutron emission strength from the fission chambers, the line integrated electron density from the 2mm interferometer [11], the electron density radial dependence from the Far Infra-Red Interferometer [12], the electron temperature radial dependence from the Electron Cyclotron Emission diagnostic [13] and the assumption that ion and electron radial dependencies are the same, then the density ratio $\hat{n}_d/\hat{n}_e$ can be determined (see Table 2).

The radial dependence of the electron temperature is much stronger than that of the electron density and therefore merits careful investigation. The ECE diagnostic [13] provides temperature profiles at very frequent intervals so as to exhibit the effect due to sawtooth oscillations. For present purposes it was appropriate to derive a profile which was the average in time over the interval during which the neutron energy spectra were accumulated, thereby suppressing all sawtooth effects. Because JET plasmas are D-shaped, a functional form for the spatial dependence of electron temperature was adopted

$$T_e(R,Z) = T_{eo}\,\Psi^p(R,Z),$$

where Ψ is a suitable paramaterization for the magnetic flux surfaces valid for low β plasmas. For circular plasmas, $T_e(R,Z) \approx T_{eo}\ (1-r^2/a^2)^{2p}$, where a is the limiter radius. Values for the peaking parameter, p, were obtained by equating the functional form to the measured radial profile at $R = R_0$ ($R_0 \simeq 3.05$m) and $R = 3.80$m, as illustrated in fig 2 for two Ohmically heated discharges. Peaking factors for all data groups of interest are plotted in fig 3 as a function of $\bar{n}_e q_\Psi$, where q_Ψ is the plasma safety factor. It is interesting to note that the peaking values for the ICRF heated discharges are double those for Ohmic discharges. It should be recognized that flux surfaces are actually contours of constant pressure so that to assume density, n_e, and temperature, T_e, are separately constant may not be entirely correct.

The density ratios from Table 2 are shown in Fig 4, plotted as a function of $\hat{T}_i$. A very strong temperature dependence is seen, with $\hat{n}_d/\hat{n}_e$ = falling from 75% at 2keV to 40% at 3keV. This result explains the low neutron yields obtained from JET for the ostensible plasma parameters achieved.

It should be appreciated that part of the decrease of the density ratio with $\hat{T}_i$ is self-inflicted owing to the practice of glow discharge cleaning with CH_4, which leads to high hydrogen concentrations in subsequent discharges, and to the use of ^{3}He as minority ion species for ICRF heating. For d-t operation neither circumstance should apply. It is therefore appropriate to introduce a new density ratio $\hat{n}_2/\hat{n}_e$, where we now derive the ratio of the sum of hydrogen, deuterium and ^{3}He ion densities to the electron density. The result is shown in Fig 5, from which it is clear that the addition of ICRF heating causes no further drop in the density ratio despite the significant temperature increase.

If the density ratio is indeed temperature dependent, it might be thought that it would be a function of the electron temperature rather than of the ion temperature. Accordingly, in Fig 6 we plot the new density ratio $\hat{n}_2/\hat{n}_e$ against $\hat{T}_e$. Not surprisingly, we find the two ICRF data points are now absorbed into the Ohmic heating points. The

pair of 4.7MA discharges (group 6) has been omitted from the plot because the current flat-top duration was insufficient for thermal equilibrium conditions between electrons and ions to be attained. The observations can be interpreted in two different ways:

(i) Lacking further input, the only safe conclusion would be that all the data points are essentially consistent with a mean value of $\hat{n}_2/\hat{n}_e$ = 0.46, or (ii) if we discard two points, that for the 4.6MA discharges on the grounds that for these $\hat{T}_i > \hat{T}_e$ (see Fig 1), which is clearly incorrect, and that for the lowest density set of discharges ($\hat{n}_e$ = 2.1 x $10^{19}m^{-3}$) on the grounds that the impurity level was conspicuously high, then we recover the temperature dependence expected from Figs 1 and 4.

6. Zeff

It is customary to determine Z_{eff} directly from bremsstrahlung measurements in the visible [14] and X-ray regions, to identify the various impurities in the plasma and thus to deduce the $\hat{n}_d/\hat{n}_e$ ratio. Because of the uncertainties in Z_{eff}, this is imprecise. Having measured the $\hat{n}_d/\hat{n}_e$ ratios, we are in a position to reverse the procedure. The resulting Z_{eff} is strictly appropriate to the central region of the plasma, whereas the bremsstrahlung measurements are volume averages.

Very little spectroscopic information is available for the discharges listed in Table 1 so we adopt the heavy impurity concentrations of 0.05% Cl and 0.05% Ni as being typical of all. The most important impurities are C and 0, which are shown to be present in the proportions 5:1 by the active charge-exchange recombination spectrometry measurements [15]; typical concentrations for Ohmically heated plasmas are 5.5% C and 1.0% 0. As these observations were not available for the discharges of present interest, we assume the balance of the electron supply after all other sources are taken into account is attributable to C and 0 in the stated proportions.

For ICRF heated discharges it is assumed that 2.5% ^{3}He is added to the

plasma (ie 5% increase in n_e). We have measured the deuterium concentrations. Finally, the hydrogen/deuterium ratio is provided by the Neutral Particle Analysis diagnostic. The resulting values for Z_{eff} are listed in Table 2, together with the visible bremsstrahlung data and values calculated from the axial plasma resistivity [16] on the assumption that $q_0 = 0.8$. In Fig 7, the Z_{eff} values deduced from the density ratios are plotted as a function of $\hat{T}_i$, a clear increase with $\hat{T}_i$ being shown.

The "neutron" Z_{eff} values are displayed in Fig 8 by group number for comparison with Z_{eff} from visible bremsstrahlung measurements and axial resistivity [16] calculations. The bremsstrahlung measurements represent volume-averaged Z_{eff} values; to obtain the required axial values a modest upwards adjustment (of perhaps 10%) should be made. It is concluded that the three Z_{eff} determinations are in fair agreement, bearing in mind their appreciable associated uncertainties.

7. Discussion

The use of neutrons for diagnostic purposes has several advantages. The measurements involve just those reactions which are at the heart of the quest for power from nuclear fusion, they are not troubled by the complexities which plague measurements on low energy radiation and neutral particle emissions and, above all, they become easier as the neutron emission strength rises. The measurement of neutron intensity is accurate and troublefree whilst the neutron energy spectra are easy to interpret for Maxwellian plasmas.

The essential experimental finding is that the high temperature Ohmically heated plasmas ($\hat{T}_i \approx 3$ keV) are heavily contaminated with impurities (known from other sources to be mainly carbon and oxygen). In addition, it appears that the impurity level at lower temperatures (2-2.5 keV) is much lower. Because of the rather large statistical uncertainties associated with the low temperature data, it is not possible to be emphatic on this point but it should be noted that the requirement that neutron yields be high for the temperature measurement to be possible means that results cannot be obtained for low temperature plasmas with high impurity levels. Thus, for the Ohmic discharges studied, a correlation between impurity level and ion

temperature is indicated but a direct ion temperature dependence is not claimed. Indeed, the observation that the addition of ICRF heating raises the ion temperature without significantly changing the impurity level demonstrates that it is the electron temperature rather than the ion temperature which may be determined by Z_{eff}.

A temperature dependence of the impurity level might be expected on the grounds that the effectiveness of Ohmic heating is directly proportional to Z_{eff}. For the high current discharges studied, the observation of sawtoothing is evidence for the safety factor q being unity in the central region of the plasma and hence the central current density (and Ohmic heating power) is independent of the total plasma current. Consequently, the relationship between the central ion temperature and the impurity level is not expected to be affected by the plasma current. Further, the observation that the increase in ion temperature due to the addition of ICRF heating is not correlated with an increase of the impurity level demonstrates that the ion temperature does not directly control the impurity level in the plasma. This finding is fully in accord with the general understanding that the impurity level in the plasma is determined by the plasma boundary conditions and that these are essentially decoupled from the conditions in the plasma centre.

References

1. M T Swinhoe and O N Jarvis, Nucl Instrum Meth in Physics Research 221 (1984) 460.

2. O N Jarvis et al. JET-IR(84)02.

3. O N Jarvis et al. JET-IR(85)06.

4. O N Jarvis et al. JET-P(86)09.

5. Jordan Valley, Emek Hayarden, Israel. Spectrometer type FNS-1.

6. G Sadler et al. Europhysics Conference Abstracts Vol 10C, Part 1 p105 (1986) and JET-P(86)15.

7. V Merlo in "Course and Workshop on Basic Physical Processes of Toroidal Fusion Plasmas", Varenna 26 August - 3 September 1985.

8. O N Jarvis et al (paper in preparation).

9. S Corti (private communication), and G Bracco et al. JET-IR(84)04.

10. E Källne (private communication).

11. J A Fessey et al. JET-P(85)04.

12. J O'Rourke et al. JET-IR(85)08.

13. A E Costley et al, "Electron Temperature Measurement on JET", Europhysics Conference Abstracts. Vol 9F, Part 1 (1985) p227.

14. P D Morgan (private communication). See also Ref 16.

15. M von Hellerman et al. Europhysics Conference Abstracts Vol 10C, Part 1, p120 (1986) and JET-P(86)15.

16. J P Christiansen "Integrated Analysis of Data for JET", JET-R(86)04.

TABLE 1

Group-Type	Pulse	B_T	I_p	$\hat{n}_e$	$\hat{T}_e$	t_s-t_f	$\hat{T}_i$ (neut)
	2852	3.4	3.3	5.0	3.7	45-51	2.32 ± .33
	2854	3.4	3.4	5.3		45-51	2.39 ± .41
1 - Ω	2855	3.4	3.4				2.97 ± .41
	2856	3.4	3.3	5.5	3.4	45-51	3.05 ± .49
	2857	3.4	3.4	5.5		45-51	3.65 ± .64
	2858	3.4	3.4	5.4	3.4	45-51	3.19 ± .52
		3.4	3.4	5.3	3.5		2.93 ± .20
	3048	3.4	3.6	5.6	3.8	44-51	3.92 ± .67
	3049	3.4	3.6	5.6	3.8		3.32 ± .49
2 - Ω	3050	3.4	3.6		3.7	45-51	3.23 ± .49
	3051	3.4	3.6	5.8	3.5		2.26 ± .34
	3052	3.4	3.5	5.9	3.5	45-50	2.59 ± .42
		3.4	3.6	5.7	3.7		3.06 ± .22
	3905	3.4	3.5	3.2	3.3		2.16 ± .44
3 - Ω	3906	3.4	3.5	3.6	3.0	46-51	2.25 ± .48
	3907	3.4	3.5	4.0	3.0	47-61	2.11 ± .42
	3908	3.4	3.5	3.8	2.8	48-51	2.28 ± .42
		3.4	3.5	3.6	3.0		2.20 ± .22
	4592	3.4	4.0	4.2	2.8	47-52	2.37 ± .45
4 - Ω	4593	3.4	4.0	4.4	2.7	47-51	2.11 ± .30
	4595	3.4	4.0	3.8		48-51	2.45 ± .37
		3.4	4.0	4.1	2.7		2.31 ± .22
	4782	3.4	4.0	3.6	3.7		3.25 ± .55
	4783	3.4	4.0	3.4	3.5	47-50	3.13 ± .54
5 - Ω	4784	3.4	4.0	3.2		46-51	3.33 ± .54
	4788	3.4	4.0	3.7	3.3	47-51	2.55 ± .41
	4791	3.4	4.0	3.8	3.2	47-51	2.42 ± .39
		3.4	4.0	3.5	3.4		2.94 ± .22

Group-Type	Pulse	B_T	I_p	n_e	T_e	t_s-t_f	T_i (neut)
	5349	3.4	4.6	3.9	3.2	46–50	2.08 ± .33
6 – Ω	5350	3.4	4.8	3.9	4.6	46–49	2.20 ± .35
		3.4	4.7	3.9	3.9		2.14 ± .25
7 – RF	6777	3.4	3.8	3.9	3.8	44–50	3.90 ± .45
	6962	2.8	3.0	2.0	3.3		
	6964	2.8	3.0	2.0	3.3		
	6965	2.8	3.0	2.1	3.3		
8 – Ω	6966	2.8	3.0	2.2	3.3		
	6967	2.8	3.0	2.2	3.3		
	6968	2.8	3.0	2.2	3.3		
	6969	2.8	3.0	2.3	3.3		
		2.8	3.0	2.1	3.3	46–52	3.06 ± .36
	7163	3.4	3.0	4.0	3.7	45–49	4.10 ± .60
	7165	3.4	3.0	3.6	4.2	45–49	5.00 ± .77
	7168	3.4	3.0	4.0	3.8	45–50	5.25 ± .71
14 – RF	7170	3.4	3.0	4.2	3.6	45–48	4.25 ± .53
	7171	3.4	3.0	3.8	3.5	45–49	3.15 ± .50
	7179	3.4	3.0	4.1	3.2	45–49	3.87 ± .71
	7180	3.4	3.0	4.0	3.5	45–48	3.75 ± .56
		3.4	3.0	4.0	3.7		4.00 ± .25
	7283	3.4	4.0	3.9	2.9	46–53	3.54 ± .55
	7284	3.4	4.5	3.9	3.0	45–53	3.58 ± .50
15 – Ω	7285	3.4	4.5	4.8	2.8	45–52	2.93 ± .36
	7287	3.4	5.0	5.2	2.7	45–53	2.99 ± .30
	7293	3.4	5.0	5.1	2.8	45–52	2.64 ± .30
		3.4	4.6	4.6	2.8		2.99 ± .16
	7607	2.8	3.0	2.5	3.3		
	7608	2.8	3.0	2.5	3.3		
16 – Ω	7611	2.8	3.0		3.3		
	7612	2.8	3.0		3.4		
	7613	2.8	3.0		3.4		
		2.8	3.0	2.5	3.3	46–52	2.37 ± .26

Notes: (i) B_T in Tesla, I_p in MA; n_e in $10^{19}m^{-3}$; T_e, T_i in keV.
(ii) Pulses 5349, 5350 did not reach equilibrium conditions.
(iii) t_s-t_f indicates start and finish times (secs) for the data acquisition.

TABLE 2

Group-Type	$\hat{n}_d/\hat{n}_e$	h/h+d	$^3He/n_e$	$\hat{n}_2/\hat{n}_e$	n_C/n_e (%)	Z_{eff}	Z_{eff}(VB)	Z_{eff}(Res)
1 - Ω	0.50 ± .05	0.05	-	0.53 ± .05	5.9 ± 0.6	3.9 ± 0.3	4.1 ± 0.7	5.0
2 - Ω	0.42 ± .08	0.05	-	0.44 ± .08	7.1 ± 1.1	4.4 ± 0.4	3.6 ± 0.6	5.2
3 - Ω	0.77 ± .15	0.03	-	0.79 ± .15	2.5 ± 2.0	2.5 ± 0.8	4.0 ± 0.6	3.5
4 - Ω	0.60 ± .14	0.03	-	0.62 ± .14	4.7 ± 1.8	3.4 ± 0.8	3.1 ± 0.5	3.0
*5 - Ω	0.46 ± .07	0.03	-	0.47 ± .06	6.7 ± 0.8	4.2 ± 0.3	3.9 ± 0.6	4.4
6 - Ω	0.71 ± .15	0.10	-	0.79 ± .15	2.5 ± 2.0	2.5 ± 0.8	3.4 ± 0.6	5.5
7 - RF	0.40 ± .11	0.05	0.025	0.45 ± .11	6.9 ± 1.4	4.4 ± 0.6	3.2 ± 0.5	3.8
8 - Ω	0.31 ± .07	0.05	-	0.33 ± .07	8.5 ± 0.9	5.0 ± 0.4	3.6 ± 0.6	4.9
14 - RF	0.35 ± .05	0.08	0.025	0.42 ± .05	7.3 ± 0.6	4.5 ± 0.3	2.9 ± 0.5	4.7
15 - Ω	0.34 ± .04	0.21	-	0.43 ± .04	7.2 ± 0.5	4.4 ± 0.3	2.6 ± 0.5	4.1
16 - Ω	0.52 ± .09	0.03	-	0.54 ± .09	5.8 ± 1.2	3.8 ± 0.5	3.0 ± 0.5	4.7
Average (less Group 6):					5.9	3.9	3.4	4.4

Systematic uncertaintiy of ± 10% in n_d/n_e has been ignored; this give additional uncertainty in Z_{eff} of ± 0.5 at Z_{eff} = 4.

Impurities: deuterium - measured
h/h+d - measured
C:O ratio = 5:1, provides balance
Cl - 0.05%
Ni - 0.05%

* Group 6 did not achieve thermal equilibrium

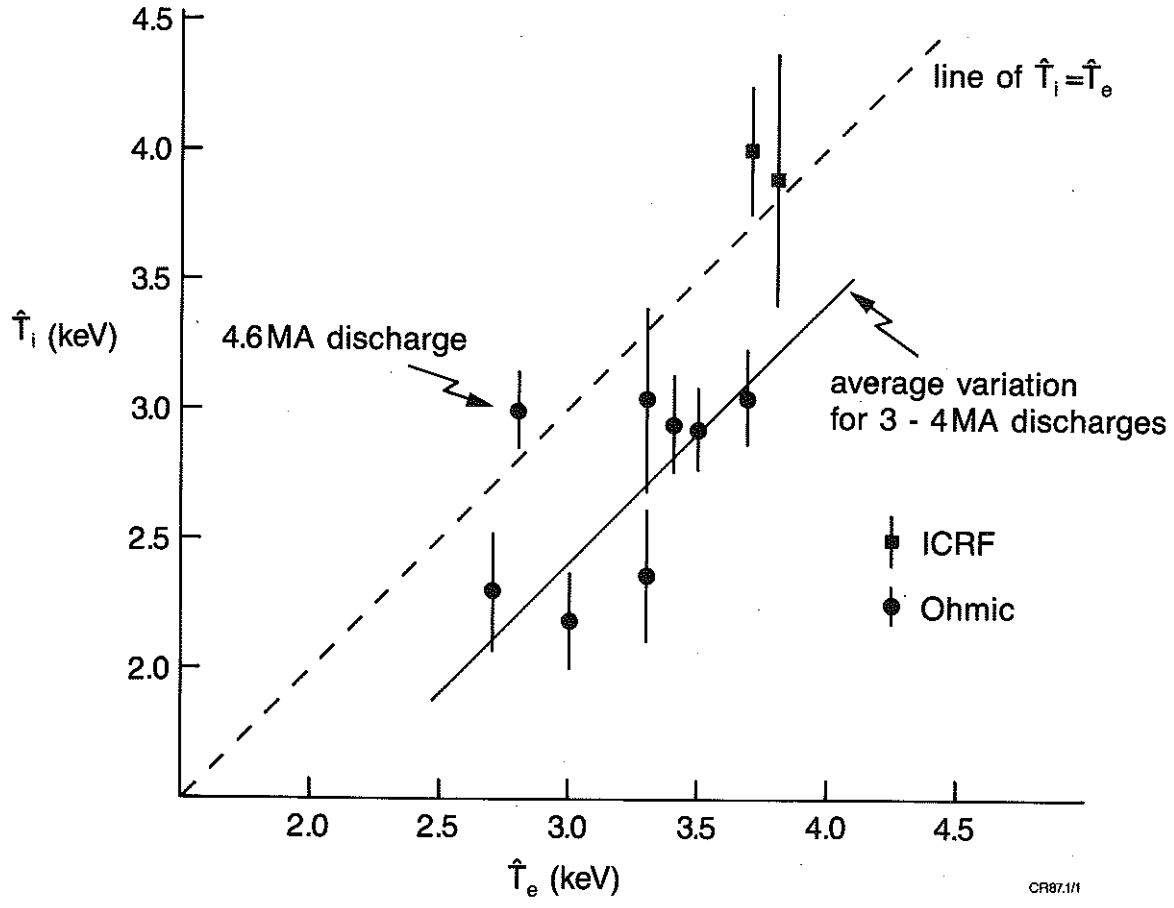

Fig 1: Showing variations of T_i with T_e for the discharges studied. Electron temperature data have ±10% normalization uncertainty. Points are plotted only for those discharges for which equilibrium conditions were obtained.

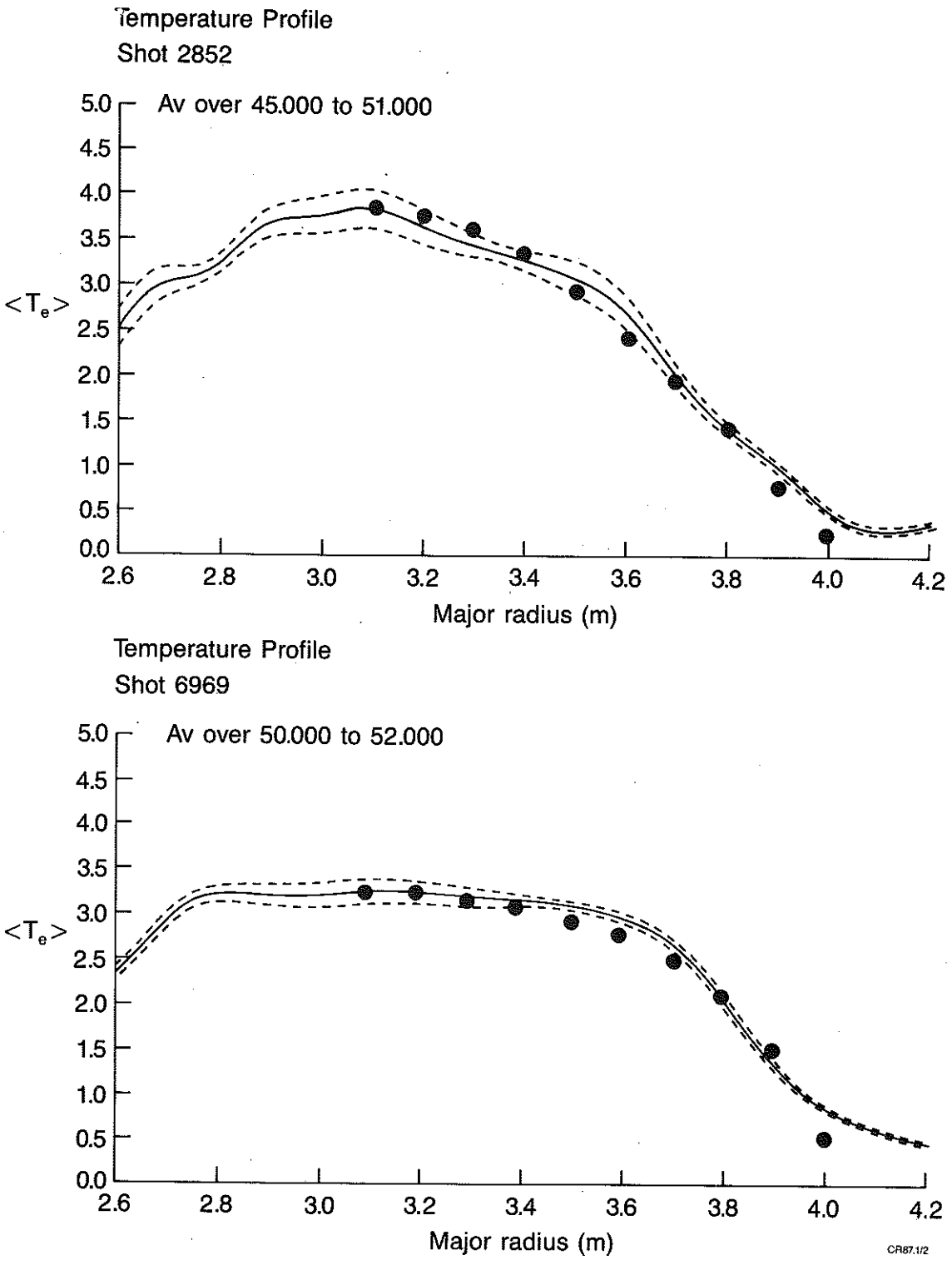

Fig 2: Electron temperature profiles. The curves show the experimental measurements and confidence levels whilst the points show the fit of the assumed functional form to the data.

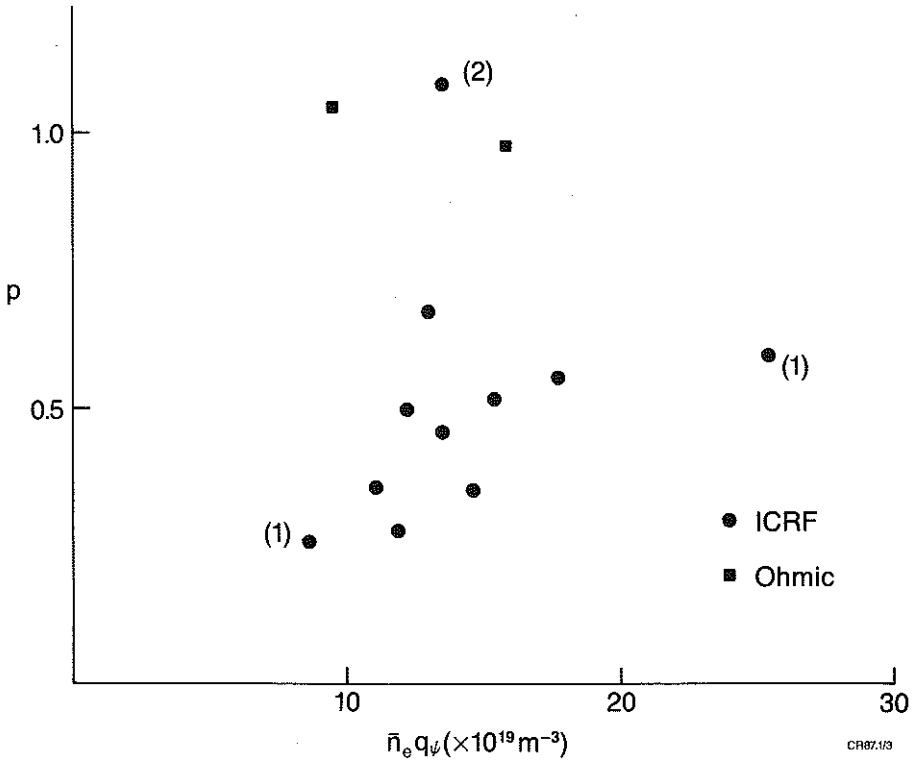

Fig 3: Peaking factor for the electron temperature radial profile, averaged over the time interval required for the ion temperature measurement.

(1) Additional points (ie. no neutron spectra).
(2) Very early data for which ECE profiles are not as reliable as for later data.

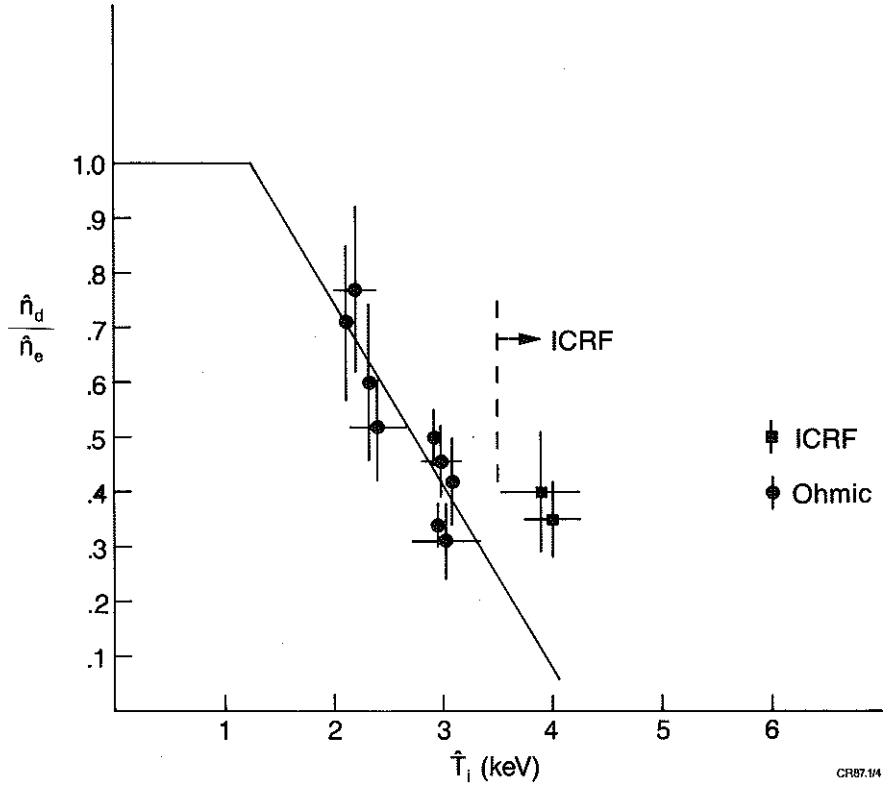

Fig 4: Variation of n_d/n_e with central ion temperature for Ohmic and ICRF (^{3}He) heating. ICRF data points not adjusted for ^{3}He addition. The line is fitted to the Ohmic points only.

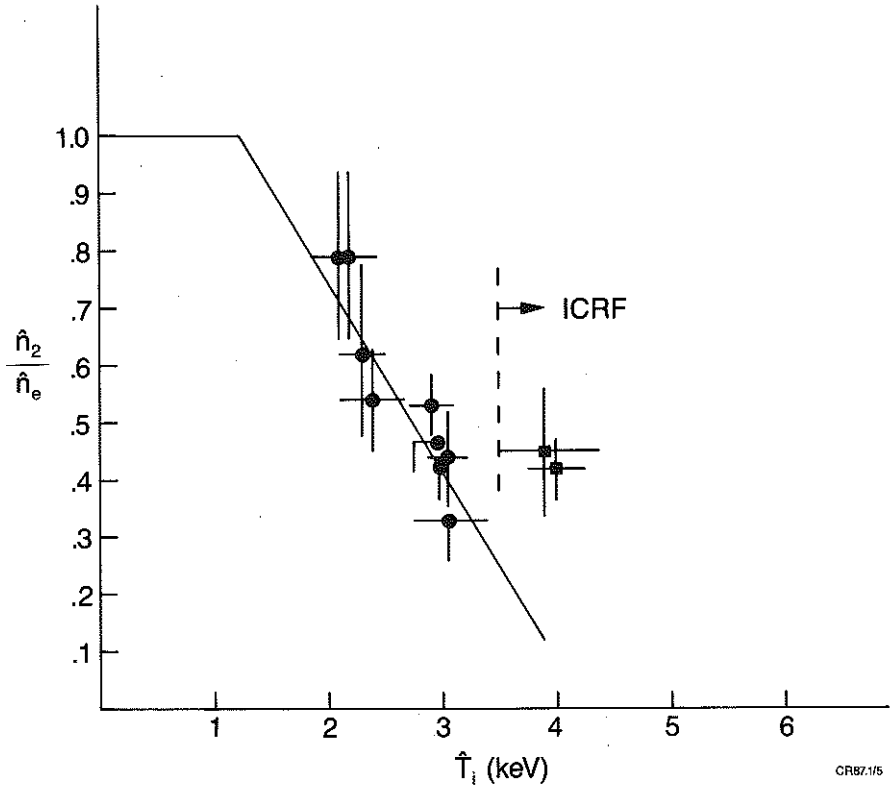

Fig 5: Variation of n_2/n_e with central ion temperature. Here, $n_2 = n_H + n_D + n_{^3He}$. The line is taken from Fig 4.

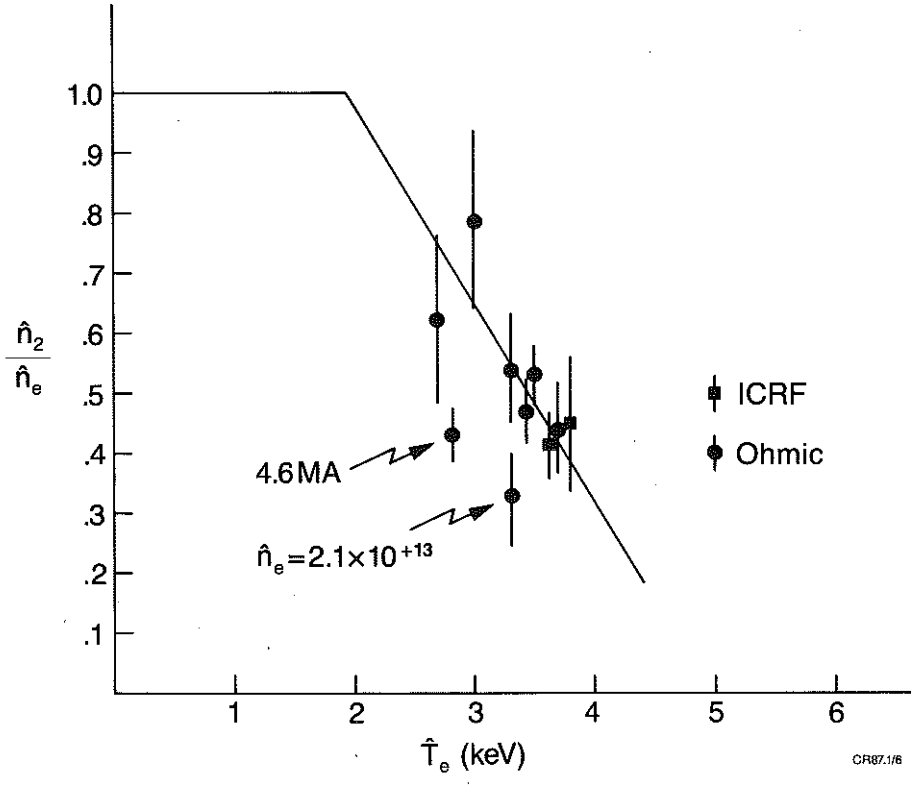

Fig 6: Variation of n_2/n_e with central electron temperature. Points are plotted only for discharges reaching equilbrium conditions. The line is as for Fig 4 with $T_e = T_i + 0.6$ keV.

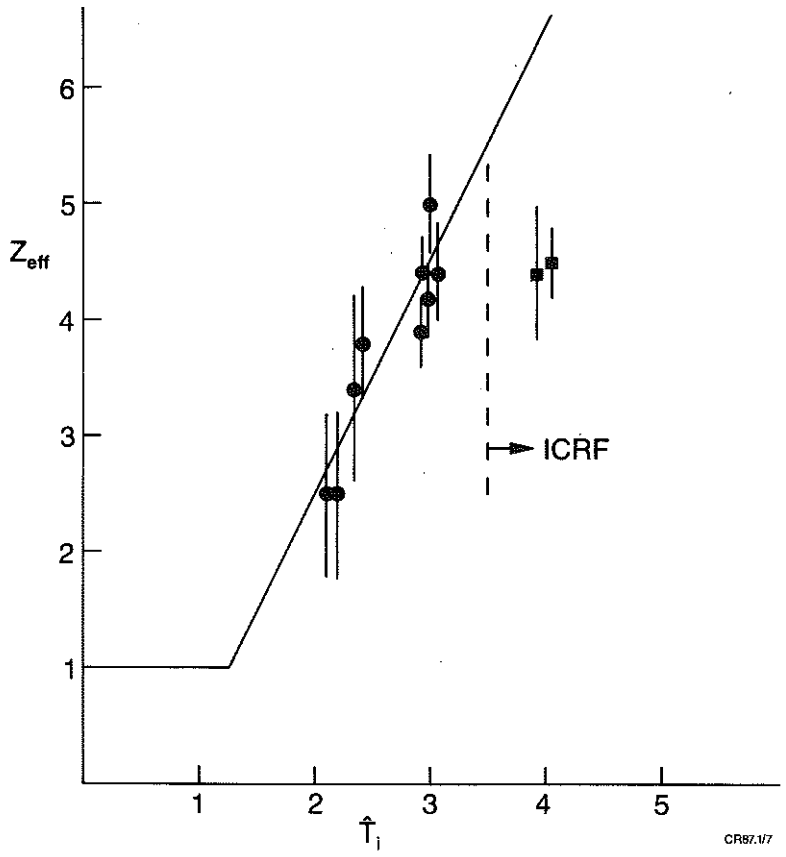

Fig 7: Showing the variation of Z_{eff} with central ion temperature. The solid line corresponds to that in Fig 4.

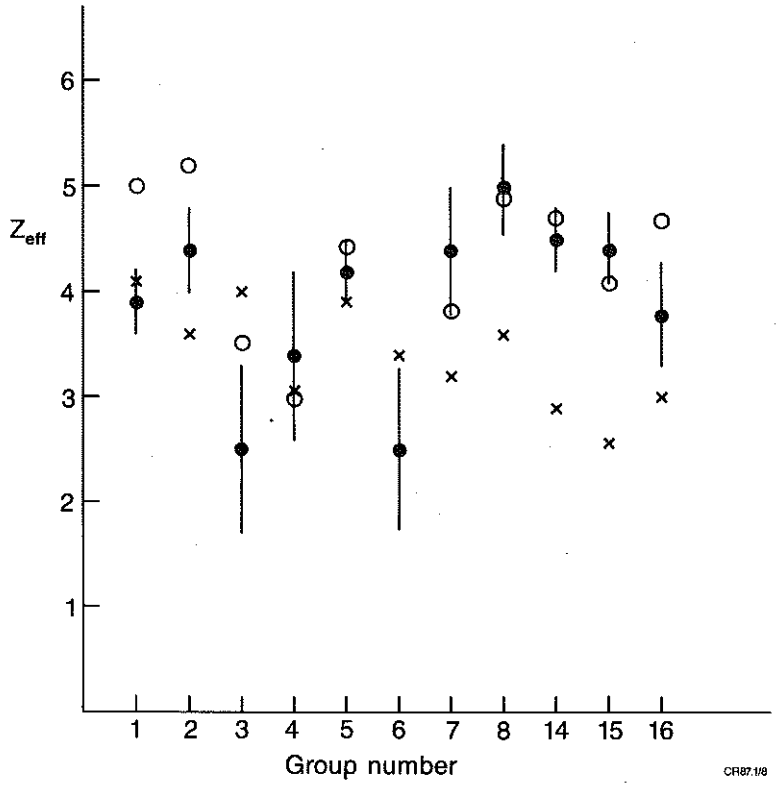

Fig 8: Comparison of Z_{eff} values obtained from neutron measurements with values from axial resistivity and visible bremsstrahlung measurements.
Φ-neutrons, X-vis brem, 0-axial resistivity.
Normalization uncertainties; ±12% neutrons, ±20% vis brem, ±25% axial resist. (q_o = 0.8).